Path Integrals Without Integrals*

Antun Balaž†, Ivana Vidanović, Aleksandar Bogojević
Scientific Computing Laboratory, Institute of Physics Belgrade
University of Belgrade, Pregrevica 118, 11080 Belgrade, SERBIA

Axel Pelster
Fachbereich Physik, Universität Duisburg-Essen
Lotharstraße 1, 47048 Duisburg, GERMANY

Abstract

Recently, we have developed an efficient recursive approach for analytically calculating the short-time expansion of the propagator to extremely high orders for a general many-body quantum system. Here we give brief overview of this approach and then demonstrate application of this technique by numerically studying the thermodynamical properties of a rotating ideal Bose gas of ^{87}Rb atoms in an anharmonic trap. The obtained results improve previous semiclassical calculations and agree well with Path Integral Monte Carlo simulations.

1. Introduction

The central object in the path-integral formulation of quantum statistics is the (Euclidean) transition amplitude $A(a,b;t) = \langle b|e^{-t\hat{H}}|a\rangle$ [1, 2, 3, 4]. The starting point in setting up this formalism is the completeness relation

$$A(a,b;t) = \int dq_1 \cdots \int dq_{N-1}\; A(a,q_1;\varepsilon)\cdots A(q_{N-1},b;\varepsilon)\,, \qquad (1)$$

where $\varepsilon = t/N$ denotes the time-slice width. To leading order in ε the short-time transition amplitude reads in natural units

$$A(q_n,q_{n+1};\varepsilon) = \frac{1}{(2\pi\varepsilon)^{d/2}} \exp\left[-\frac{(q_{n+1}-q_n)^2}{2\varepsilon} - \varepsilon V(x_n)\right], \qquad (2)$$

* This work was supported in part by the Ministry of Science and Technological Development of the Republic of Serbia, under projects No. ON141035 and ON171017 and bilateral projects PI-BEC and NAD-BEC, funded jointly with the German Academic Exchange Service (DAAD). Numerical simulations were run on the AEGIS e-Infrastructure, supported in part by FP7 project EGI-InSPIRE, HP-SEE and PRACE-1IP.

† e-mail address: antun@ipb.ac.rs

where the potential V is evaluated at the mid-point coordinate $x_n = (q_n + q_{n+1})/2$. Substituting (2) in the completeness relation (1), the deviation of the obtained discrete amplitude from the continuum result turns out to be of the order $O(\varepsilon)$. This slow convergence to the continuum is the major reason for the low efficiency of the ubiquitous Path Integral Monte Carlo simulations [5], especially in numeric studies of Bose-Einstein condensation phenomena [6, 7, 8], quantum phase transitions and phase diagrams at low temperatures [9, 10]. Thus, in order to accelerate numerical calculations for statistical properties of quantum systems, it is necessary to develop more efficient algorithms. The existence of such algorithms has been established recently [11].

To this end we worked out and numerically verified in a series of recent papers [12, 13, 14, 15] an efficient analytical procedure for improving the convergence of path integrals for single-particle transition amplitudes to the order $O(\varepsilon^p)$ for arbitrary values of p. This was achieved by studying how discretizations of different coarseness are related to a hierarchy of effective discrete-time actions which improve the convergence in a systematic way. In Ref. [16] we presented an equivalent approach which is based on a direct path-integral calculation of intermediate time amplitudes to the order $O(\varepsilon^p)$. It turned out that increasing p leads to an exponential rise in complexity of the effective actions which, ultimately, limits the maximal value of p one can practically work with. These limitations of existing approaches, in particular in the case of many-body theories, are still below the calculational barrier stemming from this rise in complexity. This is a strong indication that new and more efficient calculational schemes must exist which should considerably improve the convergence of path integrals for general many-body theories. The availability of analytic expressions for higher p effective actions is essential for numerical calculations of path integrals with high precision. Obtaining the information on energy spectra is just one important example of calculations that require high-precision numerical results. Furthermore, since the structure of higher order terms of effective actions is governed by the quantum dynamics of the system, it can be used for extracting analytical information about the system properties.

As is well known, in concrete calculations it is always easier to solve the underlying Schrödinger equation than to directly evaluate the corresponding path integral. For instance, in the case of particular potentials the Schrödinger equation approach allows an efficient recursive scheme to calculate perturbation series up to very high orders [17, 18, 19, 20, 21]. With this in mind, we have developed a new and more efficient recursive approach for deriving the short-time transition amplitude from the underlying Schrödinger equation [22]. In this paper we give an overview of this approach for one- and many-body quantum systems and then illustrate its application in the case of numerical study of properties of fast rotating Bose-Einstein condensates [23].

The paper is organized as follows: Section 2 presents the instructive case of a single one-dimensional particle moving in a general potential, while in Section 3 we extend these results to the case of a general many-body theory in d dimensions. The application of this approach to numerical calculation

of energy eigenstates and eigenfunctions by direct diagonalization of the space-discretized matrix of the evolution operator is presented in Section 4. Numerical study of properties of Bose-Einstein condensates in anharmonic traps is given in Section 5, where global and local properties such as condensation temperature, density profiles and time-of-flight absorption images are calculated for the case of fast-rotating ^{87}Rb condensate. Section 6 gives short summary of presented results and outlook for future research.

2. One particle in One Dimension

We start with calculating the transition amplitude $A(q, q'; \varepsilon)$ for one particle in one dimension. It obeys the symmetry

$$A(q, q'; \varepsilon) = A(q', q; \varepsilon) \tag{3}$$

and satisfies the time-dependent Schrödinger equations

$$\left[\frac{\partial}{\partial\varepsilon} - \frac{1}{2}\frac{\partial^2}{\partial q^2} + V(q)\right] A(q, q'; \varepsilon) = 0\,, \tag{4}$$

$$\left[\frac{\partial}{\partial\varepsilon} - \frac{1}{2}\frac{\partial^2}{\partial q'^2} + V(q')\right] A(q, q'; \varepsilon) = 0 \tag{5}$$

with the initial condition

$$A(q, q'; 0) = \delta(q - q')\,. \tag{6}$$

In terms of the deviation $\bar{x} = (q' - q)/2$ and the mid-point coordinate $x = (q + q')/2$, both equations are rewritten according to

$$\left[\frac{\partial}{\partial\varepsilon} - \frac{1}{8}\,\partial^2 - \frac{1}{8}\,\bar{\partial}^2 + \frac{1}{2}\,(V_+ + V_-)\right] A = 0\,, \tag{7}$$

$$\left[-\,\partial\bar{\partial} + 2\,(V_+ - V_-)\right] A = 0\,, \tag{8}$$

where we have introduced $V_\pm = V(x \pm \bar{x})$ as an abbreviation. Their solution may be written in the form

$$A = \frac{1}{\sqrt{2\pi\varepsilon}} \exp\left[-\frac{2}{\varepsilon}\,\bar{x}^2 - \varepsilon W(x, \bar{x}; \varepsilon)\right]\,, \tag{9}$$

where the effective potential $W(x, \bar{x}; \varepsilon)$ is an even function of $\bar{x}$ due to the symmetry (3) of the Euclidean transition amplitude. Note that Eq. (2) represents an approximation to the exact form (9) up to order $O(\varepsilon)$. Substituting (9) in (7) and (8) yields

$$W + \bar{x}\,\bar{\partial}W + \varepsilon\,\partial_\varepsilon W - \frac{1}{8}\,\varepsilon\,\partial^2 W - \frac{1}{8}\,\varepsilon\,\bar{\partial}^2 W + \frac{1}{8}\,\varepsilon^2\,(\partial W)^2 + \frac{1}{8}\,\varepsilon^2\,(\bar{\partial}W)^2 = \frac{1}{2}\,(V_+ + V_-)\,, \tag{10}$$

$$\bar{x}\,\partial W - \frac{1}{4}\,\varepsilon\,\partial\bar{\partial}W + \frac{1}{4}\,\varepsilon^2\,\partial W\bar{\partial}W = \frac{1}{2}\,(V_+ - V_-)\,. \tag{11}$$

Both partial differential equations completely determine the effective potential $W(x,\bar{x};\varepsilon)$ and thus the transition amplitude $A(q,q';\varepsilon)$. The initial condition (6) implies that W is regular in the vicinity of $\varepsilon = 0$, i.e. it may be expanded in a power series in ε. We are interested in using W to systematically speed up the convergence of discrete amplitudes with N time slices to the continuum limit. This is done by evaluating W to higher powers in ε. According to Eq. (2) the dominant term for the short-time propagation is the diffusion relation $\bar{x}^2 \propto \varepsilon$. Therefore, we expand W in a double power series in both ε and $\bar{x}^2$:

$$W(x,\bar{x};\varepsilon) = \sum_{m=0}^{\infty} \sum_{k=0}^{m} c_{m,k}(x)\, \varepsilon^{m-k} \bar{x}^{2k} \ . \tag{12}$$

Restricting the sum over m from 0 to $p-1$ leads to a discrete amplitude that converges to the continuum result as ε^p, i.e. as $1/N^p$. For later convenience we define all coefficients $c_{m,k}$, which are not explicitly used in Eq. (12), to be zero, i.e. we set $c_{m,k} = 0$ whenever the condition $m \geq k \geq 0$ is not satisfied.

Substituting the expansion (12) into the partial differential equations (10) and (11) leads to two equivalent recursion relations. The second recursion relation turns out to be more difficult to solve to higher orders as it directly determines not the coefficients $c_{m,k}(x)$ but their first derivatives. For this reason we restrict ourselves in the remainder of this section to the recursion relation following from Eq. (10). The diagonal coefficients are given by

$$c_{m,m} = \frac{V^{(2m)}}{(2m+1)!} \,, \tag{13}$$

while off-diagonal coefficients satisfy the recursion relation

$$\begin{aligned} 8(m+k+1)\, c_{m,k} &= (2k+2)(2k+1)\, c_{m,k+1} + c''_{m-1,k} - \\ &\sum_{l=0}^{m-2} \sum_{r} c'_{l,r}\, c'_{m-l-2,k-r} - \sum_{l=1}^{m-2} \sum_{r} 2\, r(2k-2r+2)\, c_{l,r}\, c_{m-l-1,k-r+1} \,, \end{aligned} \tag{14}$$

where the sum over r goes from $\max\{0, k-m+l+2\}$ to $\min\{k,l\}$ in accordance with the restriction that $c_{m,k} = 0$ whenever the condition $m \geq k \geq 0$ is not satisfied. For a given value of m, the coefficients $c_{m,k}$ for $k = 0, 1, \ldots, m$ are determined as follows. The diagonal coefficient $c_{m,m}$ is directly given by (13), whereas the off-diagonal coefficients $c_{m,k}$ follow recursively from evaluating (14) for $k = m-1, \ldots, 1, 0$.

We have automatized this procedure [24] and implemented it using the Mathematica 7 package [25] for symbolic calculus. Although the effective actions grow in complexity with level p, the Schrödinger equation method for calculating the discrete-time effective actions turns out to be extremely efficient. The whole technique can be pushed much further when working

on specific potential classes. The increase in level and the decrease in size of the expressions for the effective actions originate from functional relations between the potential and its derivatives. These relations are particularly simple in the case of polynomial interactions where all the derivatives of the potential above a certain degree vanish. However, the benefits of working within a specific class of potentials are not only limited to polynomial interactions.

As already stated, the principal rationale behind constructing high-level effective actions is to use them for speeding up Monte Carlo calculations. However, having obtained explicit expressions for effective actions to such high levels, it now becomes possible to use them extensively in both numerical and analytical calculations.

The derived effective actions can also be applied to systematically improve the Numerical Matrix Diagonalization (NMD) method [26, 27, 28] for calculating energy eigenvalues and eigenstates. Note that the propagation time t used in the NMD method is just a parameter which is chosen in such a way that it minimizes the error associated with the calculated energy eigenvalues. Therefore, it is always possible to select this parameter to be small, so that the obtained expansion of the ideal effective action can be used to substantially improve NMD calculations. Furthermore, in this case we can even use analytic $N = 1$ approximation for the path integral. In this approximation there are no integrals to perform in Eq. (1) and the amplitude is directly given by the analytic expression (9). Using such extremely rough discretizations is only possible if one has determined the ideal effective action to very high orders p. In effect, one compensates without loss of precision the increase of discretization coarseness with the input of new analytical information concerning the propagation time which is contained in the effective action. In this way, without any integration or resummation techniques, we can calculate large number of highly accurate energy eigenvalues, avoiding the usually needed limit $t \to \infty$ which is difficult to approach. When this technique is possible to use, we refer to it as $N = 1$ approximation to the path integral, or simply, calculation of path integrals without integrals.

3. Many-Body Systems

Now we extend the calculations of Section 2 to the case of a general nonrelativistic theory of M particles in d dimensions. The derivation of the equations for W proceeds completely parallel to the case of one particle in one dimension. The Schrödinger equations now have the form

$$\left[\frac{\partial}{\partial\varepsilon} - \frac{1}{2}\sum_{i=1}^{M}\triangle_i + V(q)\right] A(q,q';\varepsilon) = 0\,, \tag{15}$$

$$\left[\frac{\partial}{\partial\varepsilon} - \frac{1}{2}\sum_{i=1}^{M}\triangle'_i + V(q')\right] A(q,q';\varepsilon) = 0\,, \tag{16}$$

where $\triangle_i$ and $\triangle_i'$ stand for d-dimensional Laplacians over initial and final coordinates of particle i, while q and q' are $d \times M$ dimensional vectors representing positions of all particles at the initial and final moment. Furthermore, the potential V contains both the external potential and the respective interaction potentials between two and more particles. After substituting the dM-dimensional generalization of the expression for the transition amplitude (9) into the Schrödinger equations (15) and (16), we find the direct analogues of Eqs. (10) and (11) for the effective potential W. Either of these two equations for W can be used to determine the appropriate short-time expansion as a double Taylor series in powers of ε and even powers of $\bar{x}$:

$$W(x,\bar{x};\varepsilon) = \sum_{m=0}^{\infty} \sum_{k=0}^{m} \varepsilon^{m-k} W_{m,k}(x,\bar{x}) \;, \tag{17}$$

where $W_{m,k}(x,\bar{x}) = \bar{x}_{i_1}\bar{x}_{i_2}\cdots\bar{x}_{i_{2k}} c_{m,k}^{i_1,\ldots,i_{2k}}(x)$. It turns out to be advantageous to use recursion relations for the fully contracted quantities $W_{m,k}$ rather than the respective coefficients $c_{m,k}^{i_1,\ldots,i_{2k}}$. In this way we can avoid the computationally expensive symmetrization over all indices $i_1,\ldots,i_{2k}$. And again it is easier to work with the first of the two equations for W. Substituting (17) into the equation for the effective potential directly yields the diagonal coefficients

$$W_{m,m} = \frac{1}{(2m+1)!}(\bar{x}\cdot\partial)^{2m} V \,. \tag{18}$$

The off-diagonal coefficients satisfy the recursion relation which represents a generalization of Eq. (14):

$$\begin{aligned} 8\,(m+k+1)\,W_{m,k} &= \partial^2 W_{m-1,k} + \bar{\partial}^2 W_{m,k+1} - \\ &\sum_{l=0}^{m-2} \sum_{r} \Big[(\partial W_{l,r})\cdot(\partial W_{m-l-2,k-r}) - (\bar{\partial} W_{l,r})\cdot(\bar{\partial} W_{m-l-1,k-r+1}) \Big] \,. \end{aligned} \tag{19}$$

As before, the sum over r goes from $\max\{0, k-m+l+2\}$ to $\min\{k,l\}$. The above recursion disentangles, in complete analogy with the previously outlined case of one particle in one dimension.

4. Numerical calculation of energy eigenvalues and eigenstate

The approach presented in previous sections allows for an efficient and fast-converging numerical calculation of all one-particle properties of quantum systems [29, 30]. Note that this general numerical approach is suitable to treat arbitrarily-shaped trap potentials and is also applicable for exact studies of many-body problems. Here we consider the imaginary-time transition amplitude $A(a,b;t) = \langle b|e^{-t\hat{H}}|a\rangle$ for one particle system, where the

time t is considered to be small. If we make use of the effective action $W^{(p-1)}$ calculated to t^{p-1}, we can express this short-time amplitude as

$$A^{(p)}(a,b;t) = \frac{1}{(2\pi t)^{d/2}} \exp\Big[-\frac{2}{t}\bar{x}^2 - t\, W^{(p-1)}(x,\bar{x};t)\Big]\,, \tag{20}$$

where, as before, $\bar{x} = (b-a)/2$ and $x = (a+b)/2$. The amplitude is designated by p due to the fact that $W^{(p-1)}$ is multiplied by an additional factor of t in the exponent. This yields a result for the exponent which is correct up to order t^p, i.e. its error is proportional to t^{p+1}. If we take into account the pre-factor $1/(2\pi t)^{d/2}$, the above expression for the short time amplitude $A^{(p)}$ gives overall errors proportional to $t^{p+1-d/2}$.

If we discretize the continuous space and replace it with a grid defined by a discretization step Δ, all the quantities are defined only on a discrete set of coordinates $q_n = n\Delta$ in each dimension, where $n \in \mathbb{Z}$ is any integer number. For a physical system with Hamiltonian $\hat{H}$, the evolution operator (in the imaginary time formalism) is defined as $\exp(-t\hat{H})$, where t is the time of evolution. Transition amplitudes now define the discretized evolution operator matrix elements,

$$A_{nm}(t) = \Delta^d \cdot A(n\Delta, m\Delta; t)\,, \tag{21}$$

The eigenvectors of such a matrix correspond to the space-discretized eigenfunctions of the original Hamiltonian, while the eigenvalues are related to the eigenvalues of the Hamiltonian and can be written as

$$e^{-tE_k(\Delta,L,t)}\,, \tag{22}$$

where we emphasize the dependence of the numerically calculated eigenvalues on all discretization parameters. The number of obtained eigenvalues and eigenstates is equal to the linear size of matrix A, which has to be finite when we represent any physical system on the computer. Typically, we restrict the range of indices n, m to the finite interval $-N \le n, m < N$, so that the number of points in the grid is $S = (2N)^d$. In Eq. (22) we have also introduced the space cutoff L, which corresponds to the restriction on the range of grid-point indices n, m, and is given by $L = N\Delta$. When eigenvalues are calculated this way using the amplitudes of the order p, the appropriate errors due to the parameter t are expected to be proportional to t^p, the same as for the effective potential. In order to illustrate this, we study the quartic anharmonic oscillator with the potential

$$V(x) = \frac{1}{2}x^2 + \frac{g}{24}x^4\,. \tag{23}$$

Fig. 1 presents the analysis of various errors in the ground energy calculation for a particular choice of the parameter of the potential $g = 48$. The spectrum of the potential is calculated by the numerical diagonalization of

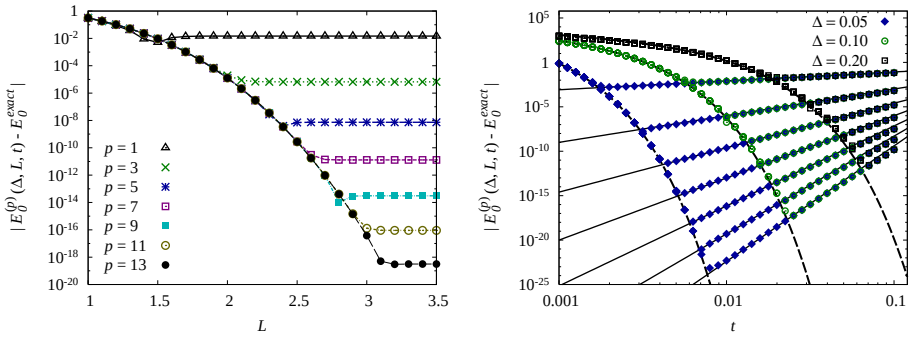

Figure 1: (a) Deviations from the ground energy $|E_0^{(p)}(\Delta, L, t) - E_0^{exact}|$ as a function of the space cutoff L and (b) as a function of the time t. The ground energy is obtained using different levels $p = 1, 3, 5, 7, 9, 11, 13$ (top to bottom) of the effective action for the quartic anharmonic potential, with parameters $g = 48$, $\Delta = 0.05$, $t = 0.02$ on graph (a), and $L = 4$ on graph (b). The exact ground energy $E_0^{exact} = 0.95156847272950001114693\ldots$ is taken from Ref. [31]. Dashed lines on the graph (b) correspond to the known discretization error [29].

the space-discretized transition amplitude matrix. The errors are estimated using the exact value of the ground energy calculated elsewhere [31] by a different technique to very high precision. The dependance of the error related to the introduction of the space cutoff L is illustrated in Fig. 1a, and is analytically known [32, 33, 29, 30]. The saturation of errors in Fig. 1a for a given level p corresponds to a maximal precision that can be achieved with that p, i.e. denotes the value of L for which errors introduced by other sources become larger than the error due to the finite value of the space cutoff. Fig. 1b gives the dependence of ground energy errors on the time of propagation parameter t for various values of the discretization step Δ. This graph clearly shows that the errors due to the time of propagation are proportional to t^p, as expected when we use level p effective action.

5. Fast Rotating Bose-Einstein Condensates

Bose-Einstein condensation (BEC) represents a macroscopic quantum phenomenon of broad research interest [34]. Since its first experimental realization in 1995, it has been extensively studied experimentally, analytically, and numerically. The two main research directions are weakly-interacting dilute gases in magneto-optical traps and strongly-interacting quantum gases in optical lattices. The behavior of a Bose-Einstein condensate under rotation is essential for understanding many fundamental BEC phenomena. For instance, its response to rotation represents one of the seminal hallmarks of superfluidity [35]. However, once a harmonically trapped Bose-Einstein condensate is rotated critically, i.e. the rotation frequency becomes so large that it compensates the radially confining harmonic frequency, the system turns out to be radially no longer trapped. In the absence of additional potential terms the condensate would start to expand perpendicular

to the rotation axis. For an overcritical rotation, this expansion would even be accelerated by the presence of a residual centrifugal force. In order to reach experimentally this delicate regime of critical or overcritical rotation, Fetter suggested in Ref. [36] to add an additional quartic term to the harmonic trap potential. Using a Gaussian laser beam propagating in the z-direction, this has been realized experimentally in Paris by Dalibard and co-workers for a BEC of $3 \cdot 10^5$ atoms of ^{87}Rb [37, 38]. The resulting axially-symmetric trap with a small quartic anharmonicity in the xy-plane, seen by individual atoms, has the form

$$V_{\mathrm{BEC}} = \frac{M_{\mathrm{Rb}}}{2}(\omega_\perp^2 - \Omega^2) r_\perp^2 + \frac{M_{\mathrm{Rb}}}{2}\omega_z^2 z^2 + \frac{k}{4} r_\perp^4 \,, \tag{24}$$

with the perpendicular radius $r_\perp = \sqrt{x^2 + y^2}$, as well as the trap frequencies $\omega_\perp = 2\pi \times 64.8$ Hz, $\omega_z = 2\pi \times 11.0$ Hz, and the trap anharmonicity $k = k_{\mathrm{BEC}} = 2.6 \times 10^{-11}$ Jm^{-4}. Furthermore, the rotation frequency Ω, which is measured in units of $\omega_\perp$, i.e. it is expressed by the ratio $r = \Omega/\omega_\perp$, represents the tunable control parameter which could be experimentally increased up to $r = 1.04$. This highest possible rotation frequency seems to coincide with an instability which follows from a Thomas-Fermi solution of the Gross-Pitaevskii equation [39].

As long as we can ignore the presence of two-particle interactions and approximately describe the system with the ideal Bose gas, its many-particle properties in the grand-canonical ensemble are exclusively derivable from one-particle states. When considering the thermodynamic limit, usually the semiclassical approximation is applied, where the one-particle ground state E_0 is retained and treated quantum mechanically, while all one-particles states above E_0 are approximately treated as a continuum [40]. This semiclassical approximation remains reasonable good irrespective of the rotation frequency Ω once the total particle number N is large enough and the trap anharmonicity k small enough. The latter condition implies that the underlying one-particle potential (24) has a small curvature around its minimum. However, in this context the question arises for which system parameters such a semiclassical approximation is not sufficient for a precise description of BEC phenomena, as well as when it finally breaks down, requiring a full quantum mechanical treatment of the system.

In order to analyze this fundamental problem more quantitatively, it is mandatory to precisely determine the one-particle energy eigenvalues and eigenfunctions, which is ideal application of our effective action approach.

5.1. Ideal Bose Gas and Path Integral Approach for BEC

For high temperatures, the grand-canonical partition function of an ideal Bose gas is given by $\mathcal{Z} = \sum_\nu e^{-\beta(E_\nu - \mu N_\nu)}$, where ν enumerates all possible configurations of the system, $\beta = 1/k_B T$ represents the inverse temperature, and μ denotes the chemical potential. As the ideal bosons do not interact, the system energy E_ν can be expressed in terms of single-particle energy eigenvalues as $E_\nu = \sum_n N_{\nu(n)} E_n$, where n counts single-particle

energy states, while $N_{\nu(n)} = 0, 1, 2, \ldots$ and E_n stand for the occupancy and the energy eigenvalue of level n, respectively. Correspondingly, the number of particles in the system is $N_\nu = \sum_n N_{\nu(n)}$ Thus, the grand-canonical free energy $\mathcal{F} = -(\ln \mathcal{Z})/\beta$ results to be

$$\mathcal{F} = \frac{1}{\beta} \sum_n \ln \left[1 - e^{-\beta(E_n - \mu)} \right] = -\frac{1}{\beta} \sum_{m=1}^{\infty} \frac{e^{m\beta\mu}}{m} Z_1(m\beta) \,, \tag{25}$$

the usual cumulant expansion. Thus, the many-body thermodynamic potential (25) of an ideal Bose gas is exclusively determined by single-particle states via the one-particle partition function $Z_1(\beta) = \sum_n e^{-\beta E_n}$.

In principle, the above outlined exact calculation of the many-body free energy allows a full numerical description of ideal Bose gases, and can be also applied for studies of dilute Bose gases in the case when interactions are negligible. However, it becomes numerically very involved even for simple trapping potentials at low temperatures. In addition to this, the BEC phase transition is achieved only in the thermodynamic limit of an infinite number of atoms, thus making numerical studies of the condensation increasingly difficult. Usually, this problem is solved by fixing the chemical potential μ at the low temperatures of the condensate phase to the ground-state energy, i.e. by setting $\mu = E_0$, and to treat the ground state separately, by explicitly taking into account its macroscopic occupation N_0. Thus, for low enough temperatures the grand-canonical free energy (25) is modified to

$$\mathcal{F} = -\frac{1}{\beta} \sum_{m=1}^{\infty} \frac{e^{m\beta\mu}}{m} \left[Z_1(m\beta) - e^{-m\beta E_0} \right] + N_0(E_0 - \mu) \,. \tag{26}$$

In order to avoid any double-counting, we have subtracted in the first line the contribution of the ground state within the one-particle partition function, whereas the second line takes into account a possible macroscopic occupation of the ground state. The resulting total number of particles $N = -\partial\mathcal{F}/\partial\mu$ follows to be

$$N = N_0 + \sum_{m=1}^{\infty} e^{m\beta\mu} \left[Z_1(m\beta) - e^{-m\beta E_0} \right] . \tag{27}$$

This particle number equation serves different purposes in the respective phases. Within the gas phase, where the macroscopic occupation of the ground state vanishes, i.e. we have $N_0 = 0$, Eq. (27) determines the temperature dependence of the chemical potential μ. On the other hand, within the BEC phase the chemical potential μ coincides with its minimal value, i.e. the ground-state energy E_0, so Eq. (27) yields the temperature dependence of N_0. Therefore, the value of $\beta_c = 1/k_B T_c$, which characterizes the boundary between both phases, follows from Eq. (27) by setting $N_0 = 0$ and $\mu = E_0$:

$$N = \sum_{m=1}^{\infty} \left[e^{m\beta_c E_0} Z_1(m\beta_c) - 1 \right] . \tag{28}$$

The conclusion is that, for a given number N of ideal bosons, the condensation temperature can be exactly calculated only if both the single-particle ground-state energy E_0 and the full temperature dependence of the one-particle partition function are known. This can be achieved by the numerical diagonalization of the one-particle Hamiltonian defined by the potential (24), using the method described in Section 4.

Typical values of the inverse temperature β in BEC experiments are quite small compared to the typical energy scale which is defined by the harmonic trap frequencies. For example, in the Paris experiment [37] the dimensionless value of $\hbar\beta\omega_\perp$ ranges between 10^{-3} and 10^{-1}. Therefore, one can immediately use the above formula for the amplitude $A^{(p)}$ and calculate the corresponding one-particle partition function by numerically integrating the diagonal amplitude $A(a, a, \beta)$ over the coordinate a. For small enough β the above formula converges rapidly, and the amplitudes can be calculated exactly for all practical purposes, i.e. using the approximation we refer to as path integrals without integrals.

However, the direct use of this approach has several disadvantages. First of all, one still has to perform an integral over the diagonal coordinate a in order to calculate the partition function. Second, this has to be done repeatedly for each value of the inverse temperature β. And most importantly, one has also to extract the value of the ground-state energy in view of the particle number equation (27). In principle, this is done by studying the high-β regime, where the short-time expansion (20) is not valid. Although this procedure works also for lower values of β [41], it requires the numerical calculation of the one-particle partition function and a detailed study of its dependence on the inverse temperature in order to obtain the ground-state energy with sufficient precision. For this reason, the algorithm becomes numerically complex and difficult to use, especially in cases where the ground state is degenerate.

The approach based on a numerical diagonalization of the space-discretized evolution operator [29, 30] effectively resolves all of the above issues. Once energy spectra is calculated in the low-β regime, this can be used to obtain the one-particle partition function for any value of the inverse temperature β in a numerically inexpensive way. Calculations based on this approach do not have restrictions in the high-β regime, where, in fact, they turn out to yield results with even better precision. In addition, the one-particle energy eigenfunctions obtained by the exact diagonalization will allow us to calculate local properties of Bose-Einstein condensates with very high accuracy.

This procedure is implemented in Fig. 2 for several values of the rotation frequency Ω in units of $r = \Omega/\omega_\perp$. For example, from Fig. 2a for $T_c = 63.14$ nK we see that the corresponding number of particles is $N = 3 \cdot 10^5$, which coincides with the value for a critically rotating condensate in the experiment of Dalibard and co-workers [37]. Fig. 2b summarizes the numerical results for the condensation temperature T_c for the anharmonicity $k = k_{\mathrm{BEC}}$ as well as the particle numbers $N = 3 \cdot 10^5$ and $N = 1 \cdot 10^4$. If we compare the obtained numerical results with the semiclassical approximation from

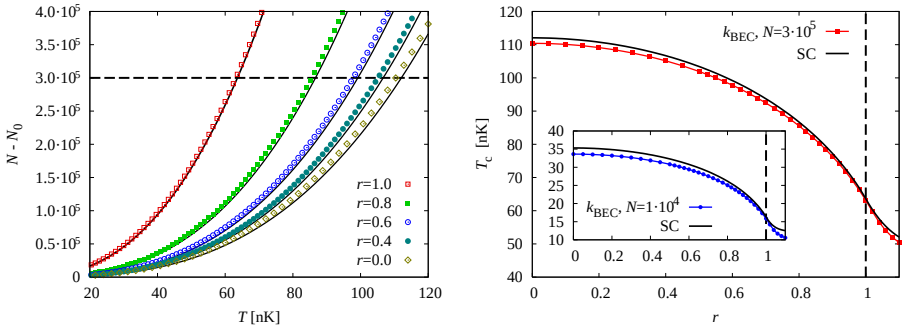

Figure 2: (a) Number of thermally excited atoms $N - N_0$ as a function of the temperature T for different values of the rotation frequency and the quartic anharmonicity $k = k_{\mathrm{BEC}}$. The dashed line corresponds to the number of atoms $N = 3 \cdot 10^5$ in the experiment [37]. (b) The condensation temperature as a function of the rotation frequency for the condensate of $N = 3 \cdot 10^5$ and $N = 1 \cdot 10^4$ atoms of ^{87}Rb, with the quartic anharmonicity of the trap $k = k_{\mathrm{BEC}}$. For comparison, the full lines on both graphs depict the semiclassical results from Ref. [40].

Ref. [40], we see that the agreement turns out to be relatively good for the undercritical regime, but it becomes worse for an overcritical rotation of the condensate. Note that semiclassical corrections due to higher region of energy spectra [23] is also taken into account in our numerical calculations.

5.2. Density Profiles and Time-of-Flight Graphs

The two-point propagator $\rho(x_1, x_2) = \langle \hat{\Psi}^\dagger(x_1)\hat{\Psi}(x_2)\rangle$ defines via its diagonal element, i.e. $n(x) = \rho(x, x)$, the density profile of atoms in a trap. For the ideal Bose gas, the density profile can be written as

$$n(x) = N_0|\psi_0(x)|^2 + \sum_{n\geq 1} N_n|\psi_n(x)|^2\,, \tag{29}$$

where the second term represents the thermal contribution to the density profile. Furthermore, the quantities ψ_n represent single-particle eigenstates, while the occupancies N_n with $n \geq 1$ are given by the Bose-Einstein distribution

$$N_n = \frac{1}{e^{\beta(E_n - E_0)} - 1}\,. \tag{30}$$

Having at our disposal numerically calculated energy eigenvalues and eigenfunctions, we can calculate the density profile of the condensate. In order to do so, we first have to obtain the ground-state occupancy number N_0 using the approach described in the previous section. Once this is done, Eq. (29) allows to calculate the density profile. In view of a comparison with absorption imaging, which always produces two-dimensional profiles, we have to integrate our numerically determined three-dimensional particle density $n(x)$ along the imaging axis z. Fig. 3 presents typical results

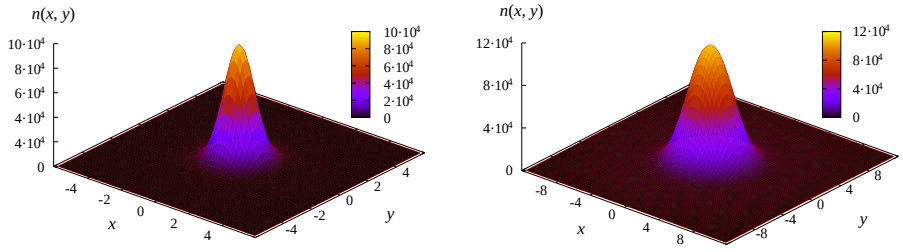

Figure 3: Density profile in xy-plane for a non-rotating (top) and a critically rotating (bottom) condensate of $N = 3 \cdot 10^5$ atoms of ^{87}Rb with the anharmonicity $k = k_{\mathrm{BEC}}$ at $T = 30$ nK. The dimensionless unit length on both graphs corresponds to 1.34 μm, i.e. the linear size of the profile is approximately 16.1 μm (left) and 32.2 μm (right).

for the resulting density profiles of Bose-Einstein condensates for both the non-rotating and the critically-rotating case. Obviously, a rotation of the condensate leads to an effective spreading due to the appearance of a centrifugal potential.

Although this approach is sufficient for treating the low-temperature regime, where the condensate is present, we emphasize that the same method can also be used to deal with the thermal regime, when the temperature is increased beyond T_{c}. For even higher temperatures, when the number of energy eigenstates, that need to be taken into account, exceeds the number of numerically accessible eigenstates, the presented approach can be extended in a similar way as the partition function was calculated previously as a sum of diagonal transition amplitudes. Using the cumulant expansion of occupancies and the spectral decomposition of thermal transition amplitudes, the density profile can be written for high enough temperatures as

$$n(x) = N_0|\psi_0(x)|^2 + \sum_{m\geq 1}\left[e^{m\beta E_0}A(x,0;x,m\beta) - |\psi_0(x)|^2\right]. \qquad (31)$$

Here $A(x,0;x,m\beta)$ represents the imaginary-time amplitude for a single-particle transition from the position x in the initial imaginary time $t = 0$ to the position x in the final imaginary time $t = m\beta$.

While both definitions (29) and (31) are mathematically equivalent in the case when one is able to calculate infinitely many energy eigenstates and amplitudes for an arbitrary propagation time, the first one is more suitable for low temperatures, when the number of relevant energy eigenstates is moderate, and the second one is suitable for high temperatures, when the imaginary propagation time β is small, and the short-time expansion can be successfully applied.

In typical BEC experiments, a trapping potential is switched off and the gas is allowed to expand freely during a short flight time t which is of the order of several tens of milliseconds. Afterwards an absorption picture is

taken which maps the density profile to the plane perpendicular to the laser beam. For the ideal Bose condensate, the density profile after time t is given by

$$n(x,t) = N_0|\psi_0(x,t)|^2 + \sum_{n\geq 1} N_n|\psi_n(x,t)|^2\,, \tag{32}$$

where the density profile has to be integrated along the imaging axis, and the eigenstates $\psi_n(x,t)$ are propagated according to the free Hamiltonian, containing only the kinetic term, since the trapping potential is switched off. If the energy eigenstates are available exactly, either analytically or numerically, their propagation time can be calculated by performing two consecutive Fourier transformations:

$$\psi_n(x,t) = \int \frac{d^3k\, d^3R}{(2\pi)^3}\, e^{i[k\cdot(r-R)-\omega_k t]}\, \psi_n(R)\,, \tag{33}$$

where the term $e^{-i\omega_k t}$ accounts for a free-particle propagation in k-space. In practical applications, when the energy eigenstates are calculated by a numerical diagonalization of space-discretized transition amplitudes, the natural way to calculate the above free-particle time evolution is to use Fast Fourier Transform (FFT) numerical libraries. This is illustrated in Fig. 4 for overcritical rotation.

For high temperatures we can use a mathematically equivalent definition of the density profile which is derived again from using the cumulant expansion of occupancy numbers and the spectral decomposition of transition

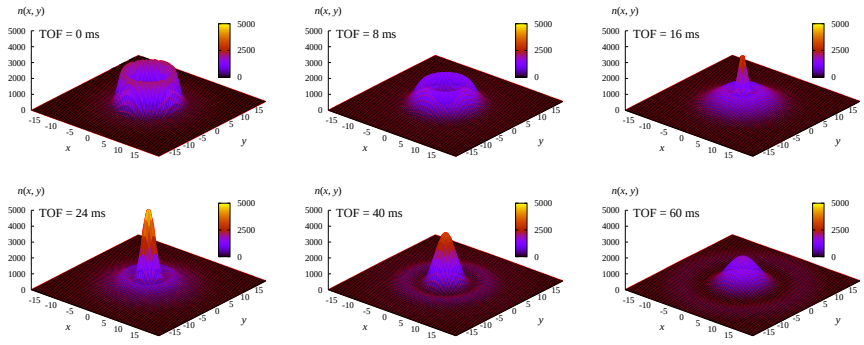

Figure 4: Time-of-flight absorption density profiles in xy-plane for an over-critically rotating ($r = 1.04$) condensate of $N = 3\cdot 10^5$ atoms of ^{87}Rb with the anharmonicity $k = k_{\mathrm{BEC}}$ at $T = 30$ nK. The flight time, designated as TOF, is given at each plot. The dimensionless unit length on all graphs corresponds to 1.34 μm and the linear size of profiles is approx. 53.6 μm.

amplitudes:

$$n(x,t) = N_0|\psi_0(x,t)|^2 + \sum_{m\geq 1}\left[e^{m\beta E_0}\int \frac{d^3k_1\, d^3k_2\, d^3X_1\, d^3X_2}{(2\pi)^6} \times \right.$$
$$\left. e^{i[(k_1-k_2)\cdot x - k_1\cdot X_1 + k_2\cdot X_2 - (\omega_{k_1}-\omega_{k_2})t]} A(X_1,0;X_2,m\beta) - |\psi_0(x,t)|^2\right]. \quad (34)$$

In both approaches it is first necessary to calculate the ground-state energy E_0 and the eigenfunction $\psi_0(x)$, as well as the ground-state occupancy N_0. If we rely on Eqs. (32) and (33) to calculate time-of-flight graphs, we have to calculate as many eigenstates as possible by numerical diagonalization. Conversely, if it is possible to use directly Eq. (34), we can apply the effective action short-time exp

6. Conclusions and Outlook

We have presented an analytic procedure for determining the short-time propagation of a general non-relativistic M-particle theory in d dimensions to extremely high orders. The procedure is based on recursively solving the Schrödinger equation for the transition amplitude in a power series of the propagation time. This leads to a new recursion relation that can be solved to the desired order p. The presented results define the state-of-the-art for calculating short-time expansion amplitudes. They can be used to obtain orders of magnitude speedup in Path Integral Monte Carlo calculations.

This approach is applied for an efficient numerical calculation of both global and local properties of fast-rotating Bose-Einstein condensates. To this end we have calculated large numbers of single-particle eigenvalues and eigenstates using an exact numerical diagonalization of the space-discretized evolution operator matrix. Using this information, we have calculated the condensation temperature and the ground-state occupancy of the condensate, as well as density profiles and time-of-flight absorption graphs.

We plan to continue development of this approach and to extend it to systems with time-dependent potentials, as well as to the case of real-time dynamics. We also plan to derive higher-order estimators for numerical calculation of the expectation values of kinetic and potential energy, heat capacity, and susceptibility.

References

[1] R. P. Feynman, Rev. Mod. Phys. **20**, 367 (1948).

[2] R. P. Feynman, and A. R. Hibbs, *Quantum Mechanics and Path Integrals*, McGraw-Hill, New York, 1965.

[3] R. P. Feynman, *Statistical Mechanics*, W. A. Benjamin, New York, 1972.

[4] H. Kleinert, *Path Integrals in Quantum Mechanics, Statistics, Polymer Physics, and Financial Markets*, 5th ed. (World Scientific, Singapore, 2009).

[5] D. M. Ceperley, Rev. Mod. Phys. **67**, 279 (1995).

[6] S. Pilati, K. Sakkos, J. Boronat, J. Casulleras, and S. Giorgini, Phys. Rev. A **74**, 043621 (2006).

[7] C. Zhang, K. Nho, and D. P. Landau, Phys. Rev. A **77**, 025601 (2008).

[8] S. Pilati, S. Giorgini, and N. Prokof'ev, Phys. Rev. Lett. **100**, 140405 (2008).

[9] E. Vitali, M. Rossi, F. Tramonto, D. E. Galli, and L. Reatto, Phys. Rev. B **77**, 180505(R) (2008).

[10] D.-H. Kim, Y.-C. Lin, and H. Rieger, Phys. Rev. E **75**, 016702 (2007).

[11] C. Predescu, Phys. Rev. E **69**, 056701 (2004).

[12] A. Bogojević, A. Balaž, and A. Belić, Phys. Rev. Lett. **94**, 180403 (2005).

[13] A. Bogojević, A. Balaž, and A. Belić, Phys. Rev. B **72**, 064302 (2005).

[14] A. Bogojević, A. Balaž, and A. Belić, Phys. Lett. A **344**, 84 (2005).

[15] A. Bogojević, A. Balaž, and A. Belić, Phys. Rev. E **72**, 036128 (2005).

[16] A. Bogojević, I. Vidanović, A. Balaž, and A. Belić, Phys. Lett. A **372**, 3341 (2008).

[17] C. M. Bender and T. T. Wu, Phys. Rev. **184**, 1231 (1969); Phys. Rev. D **7**, 1620 (1973).

[18] W. Janke and H. Kleinert, Phys. Rev. Lett. **75**, 2787 (1995).

[19] F. Weissbach, A. Pelster, and B. Hamprecht, Phys. Rev. E **66**, 036129 (2002).

[20] S.F. Brandt, H. Kleinert, and A. Pelster, J. Math. Phys. **46**, 032101 (2005).

[21] J. Dreger, A. Pelster, and B. Hamprecht, Europ. Phys. J. B **45**, 355 (2005).

[22] A. Balaž, A. Bogojević, I. Vidanović, A. Pelster, Phys. Rev. E **79**, 036701 (2009).

[23] A. Balaž, I. Vidanović, A. Bogojević, A. Pelster, Phys. Lett. A **374**, 1539 (2010).

[24] SPEEDUP Mathematica and C code, `http://www.scl.rs/speedup`

[25] Mathematica software package, `http://www.wolfram.com/mathematica`

[26] E. L. Pollock and D. M. Ceperley, Phys. Rev. B **30**, 2555 (1984).

[27] A. Sethia, S. Sanyal, and Y. Singh, J. Chem. Phys. **93**, 7268 (1990).

[28] A. Sethia, S. Sanyal, and F. Hirata, Chem. Phys. Lett. **315**, 299 (1999).

[29] I. Vidanović, A. Bogojević, A. Belić, Phys. Rev. E **80**, 066705 (2009).

[30] I. Vidanović, A. Bogojević, A. Balaž, A. Belić, Phys. Rev. E **80**, 066706 (2009).

[31] W. Janke, H. Kleinert, Phys. Rev. Lett. **75**, 2787 (1995).

[32] G. Barton, A. J. Bray, A. J. McKane, Am. J. Phys. **58**, 751 (1990).

[33] D. H. Berman, Am. J. Phys. **59**, 937 (1991).

[34] L. Pitaevskii and S. Stringari, *Bose-Einstein Condensation* (Oxford University Press, Oxford, 2003).

[35] A. L. Fetter, Rev. Mod. Phys. **81**, 647 (2009).

[36] A. L. Fetter, Phys. Rev. A **64**, 063608 (2001).

[37] V. Bretin, S. Stock, Y. Seurin, and J. Dalibard, Phys. Rev. Lett. **92**, 050403 (2004).

[38] I. Bloch, J. Dalibard, and W. Zwerger, Rev. Mod. Phys. **80**, 885 (2008).

[39] S. Kling and A. Pelster, Laser Physics **19**, 1072 (2009).

[40] S. Kling and A. Pelster, Phys. Rev. A **76**, 023609 (2007).

[41] D. Stojiljković, A. Bogojević, and A. Balaž, Phys. Lett. A **360**, 205 (2006).